

invited paper for
"Chinese Journal of Semiconductors"
this is a rewrite of previous conference papers

High Power SiGe X-Band (8-10 GHz) Heterojunction Bipolar Transistors and Amplifiers

Zhenqiang Ma^{1*}, Guogong Wang¹, Ningyue Jiang¹,

George E. Ponchak² and Samuel A. Alterovitz²

¹Department of Electrical and Computer Engineering, University of Wisconsin-Madison

Madison, WI 53706, USA

²NASA-Glenn Research Center, Cleveland, OH 44135, USA

*Corresponding author:

Prof. Zhenqiang (Jack) Ma
University of Wisconsin-Madison
1415 Engineering Drive
Room 3445 EH
Madison, WI 53706
USA
Phone: (608) 261-1095
Fax: (608) 262-1267
Email: mazq@engr.wisc.edu

Abstract

Limited by increased parasitics and thermal effects as the device size becomes large, current commercial SiGe *power* HBTs are difficult to operate at X-band (8-12 GHz) with adequate power added efficiencies at high power levels. We found that, by changing the heterostructure and doping profile of SiGe HBTs, their power gain can be significantly improved without resorting to substantial lateral scaling. Furthermore, employing a common-base configuration with proper doping profile instead of a common-emitter configuration improves the power gain characteristics of SiGe HBTs, which thus permits these devices to be efficiently operated at X-band. In this paper, we report the results of SiGe power HBTs and MMIC power amplifiers operating at 8-10 GHz. At 10 GHz, 22.5 dBm (178 mW) RF output power with concurrent gain of 7.32 dB is measured at the peak power-added efficiency of 20.0% and the maximum RF output power of 24.0 dBm (250 mW) is achieved from a 20 emitter finger SiGe power HBT. Demonstration of single-stage X-band medium-power linear MMIC power amplifier is also realized at 8 GHz. Employing a 10-emitter finger SiGe HBT and on-chip input and output matching passive components, a linear gain of 9.7 dB, a maximum output power of 23.4 dBm and peak power added efficiency of 16% is achieved from the power amplifier. The MMIC exhibits very low distortion with 3rd order intermodulation (IM) suppression C/I of -13 dBc at output power of 21.2 dBm and over 20dBm 3rd order output intercept point (OIP3).

Index Terms: Common-base (CB), common-emitter (CE), doping profile, load-pull, MMIC, power amplification, power gain, SiGe heterojunction bipolar transistors (HBTs).

I. INTRODUCTION

The fast advances of SiGe HBT technology have enabled many high frequency microwave circuits to be built on Si substrates. However, medium and high power amplifiers operated at X-band and higher frequencies have not been successfully developed using commercial SiGe HBTs. This is due to the fact that using the current SiGe HBT structure (low Ge content) and doping profile (high-to-low from emitter to base) limits the power gain of large area SiGe HBTs at X-band frequencies. As the device area increases, the power gain values further degrade due to increased parasitics (including the added ballast resistors) and thermal effects. As a result, while these commercial SiGe HBTs are capable of operating in the frequency range of from 1.9 GHz to 5.3 GHz [1], they become incapable of power amplification beyond 8 GHz. It is found that with proper design of the SiGe HBT structure and doping profile the power gain values of these devices can be dramatically improved without involving submicron lateral scaling or sacrificing breakdown voltage characteristics. In addition, by employing the proper configuration, much higher power performance can be extracted from SiGe HBTs with properly designed structures. In this paper, we report the performance characteristics of SiGe power HBTs and medium-power MMIC power amplifiers operating at 8-10 GHz.

II. SiGe HBT DESIGN AND OPERATION CONFIGURATION CONSIDERATIONS

To achieve a high maximum frequency of oscillation, f_{\max} , (>40-50GHz) such that sufficient power gain is available at 8-10 GHz while maintaining high breakdown voltage (required for ruggedness of power amplifiers) and relaxing the lithography restriction for lowering the fabrication cost, the most efficient method is to reduce the base resistance, R_B , by increasing the base doping concentration of SiGe power HBTs. However, the prevalent trapezoidal Ge profile with low Ge content employed in commercial SiGe HBTs sets a limit for the maximum allowable doping concentration in the base. Alternatively, by increasing the Ge composition

near the base-emitter (B-E) junction to change the trapezoidal profile into a box-type one with a higher total Ge content, the doping concentration in the base region can be much higher than currently used. The reduction of R_B resulting from using a heavily doped base region can significantly boost the f_{\max} values without deep submicron scaling of the emitter stripe widths. As a result, high power gain can be achieved at higher frequencies by employing a box-type Ge profile with a heavily doped base region.

In the heterostructure design of the SiGe power HBTs, the collector epilayer is made thick (0.5 μm) and lightly doped ($3 \times 10^{16} \text{cm}^{-3}$) to realize a high breakdown voltage. The box-type Ge profile (21%) is used to maintain a large valence band offset between the emitter and the base. This box-type Ge profiles thus permits a high boron, B, doping concentration ($2.5 \times 10^{19} \text{cm}^{-3}$) to be employed in the base region with sufficient DC current gain values ($\beta=30$). Due to the heavy doping concentration, a low base sheet resistance ($\sim 3 \text{k}\Omega/\square$, much lower than any reported values from commercial SiGe HBTs) can be achieved, even with a thin (32 nm) base region. In addition, the emitter finger width can still be large without inducing serious emitter current crowding effect due to reduced base sheet resistance. The SIMS analysis results of the heterostructure are shown in Fig. 1.

A uniformly distributed subcell structure (with two $2 \times 30 \mu\text{m}^2$ emitter fingers in each subcell) is used in this power device layout and detailed structure can be found in a previous paper [2]. Fig. 2 shows the 10-finger device with a total emitter area of $600 \mu\text{m}^2$. The power devices were processed on 0.5 mm-thick Si substrates and no external ballast resistors or substrate thinning was employed. The one-step CVD-grown heterostructures were fabricated into mesa-type HBTs.

The device operation configuration also needs to be reconsidered for power amplifications at 8-10 GHz. To date, the common-emitter (CE) configuration has been generally employed for power amplifications for SiGe HBTs (*e.g.*, 1.9-2.4 GHz) integrated in SiGe BiCMOS. Nevertheless, our recent study [3] shows that for SiGe HBTs having a typical Si bipolar junction

transistor (BJT) doping profile in conjunction with a trapezoidal Ge profile the CE configuration always offers higher power gain (G_{\max}) than the common-base (CB) configuration in the low operation frequency range (e.g., <6 GHz) [3]. As a result, the common practice using the CE configuration for these SiGe HBTs in the 1.9-5.3 GHz is justified. However, at higher operation frequencies, no matter what type of doping profiles and Ge profiles is used for SiGe HBTs, the CB configuration tends to provide higher G_{\max} values than the CE configuration [3]. Furthermore, we also revealed that with a small value of (total) base resistance, which can be effectively made possible with a heavy base doping concentration as described earlier, a higher G_{\max} can be obtained from the CB than from the CE configuration over a wider frequency range. Therefore, for SiGe HBTs employing a heavily doped base region, the CB configuration ought to be judiciously considered for power amplifications at 8-10 GHz (contrary to common practice). Fig. 3 shows the measured power gain (G_{\max}) characteristics of 10-emitter finger SiGe HBTs under CE and CB configurations, respectively. Due to the heavy base doping concentration employed in the heterostructure (Fig. 1), which is permitted by employing a box type Ge profile with high Ge content, a small base resistance is achieved and thus, in a wide frequency range (measured frequency range: 2-40 GHz), the CB configuration provides higher power gain values than the CE configuration.

III. POWER HBT PERFORMANCE AT 8 AND 10 GHz

The power performance of a 20-finger CB SiGe HBT was tested on wafer at 10 GHz using a single-tone Focus Microwave load-pull system under class-AB operation in continuous wave (CW) mode. No special arrangement for heat dissipation was employed in the measurements. The device was biased at $V_{EB}=-0.9V$ and $V_{CB}=6V$ (class-AB), and the source ($\Gamma_S = 0.77\angle 185^\circ$) and load ($\Gamma_L = 0.78\angle 141^\circ$) matching were optimized for maximum output power. The measured output power P_{out} , gain and PAE are plotted as a function of input power P_{in} in Fig. 4.

The measured linear gain is 9.37 dB. At 1- and 3-dB gain compression, the RF output power $P_{-1\text{dB}}$ and $P_{-3\text{dB}}$ are 21.2 dBm (132 mW) and 23.1 dBm (204 mW), respectively. The maximum PAE, i.e., 20.0%, is achieved at 2-dB gain compression with associated RF output power of 22.5 dBm (178 mW). The largest RF output power that the device can generate is 24.0 dBm (251 mW, $0.21\text{-mW}/\mu\text{m}^2$ power density). Higher PAE could be obtained if the measurement is optimized for highest PAE. No thermal or electrical instability was observed under these operating conditions. The thermal stability is mainly ascribed to the high thermal conductivity of the silicon substrate and due to the distributed layout design [2].

For comparison, the power performance of the same device operating at 8 GHz is also measured and the result is shown in Fig. 5. The device exhibits 22.7 dBm (186 mW) RF output power with concurrent gain of 8.65 dB at the peak power-added efficiency (25.3%). Higher power performance measured at 8 GHz is due to the improved power gain at lower frequencies as shown in Fig. 3. Due to much lower power gain values at 8 and 10 GHz for CE configuration (Fig. 3), large-signal power performance could not be measured, indicating the necessity of employing a proper configuration. Therefore, it is evident that the power amplification frequency is extended by using CB configuration. It is noted, furthermore, that the CB configuration can effectively extend the operation frequency when a low base resistance is realized (by employing a high Ge content with box shape and heavy doping level in the base region).

IV. ON-CHIP SPIRAL INDUCTORS AND SiO MIM CAPACITORS

The passive components, including spiral inductors and MIM capacitors, are important circuit components that are used as matching elements, bias chokes and filter components. The lumped form of these components has the advantage of smaller form factor than the distributed transmission line components at 8-10 GHz. The quality factor, which is limited by the parasitic resistance and capacitance (for inductors) or parasitic inductance (for capacitors), of these

components directly affect the matching circuit design and power amplifier performance. In particular, the series resistance associated with spiral inductors can substantially degrade the power performance of power amplifiers. Fortunately, in modern SiGe BiCMOS process, the thick copper technology used in the top levels of multilevel interconnects along with the advances of “winding” techniques has greatly alleviated this issue. In this study, the lumped inductors, consisting of Ti/Al/Ti/Au/Ni (2.5 μ m thick) films, were made on top of 1 μ m PECVD oxide deposited on high-resistivity Si substrates. The frequency of resonance of these spiral inductors was improved using isotropic deep RIE etch to remove the majority of material underneath the metal lines and reduce the parasitic capacitance associated with the inductors. The resulting inductors demonstrate a quality factor of 12-16 with over 30 GHz resonance frequencies, depending on the size of the inductors. The MIM capacitors, consisting of an evaporated SiO₂ dielectric layer sandwiched between top metal Ti/Al/Ti/Au/Ni and bottom metal Ti/Au (same as the center conductor of the spiral inductors), exhibit quality factor over 40 and resonance frequency of over 40 GHz after deep RIE etch. The processing techniques used here are similar to these described previously [4].

IV. LINEAR MMIC MEDIUM POWER AMPLIFIER DEMONSTRATION AT 8GHz

A single-stage power amplifier circuit was designed using the large-signal model of SiGe HBTs and passive components models (extracted and verified with measured S-parameters). The on-chip input and output matching networks were designed for high output power and both were matched to 50-ohm impedance. In order to achieve high linearity with the available passive components, a simple L-C short circuit was implemented at the output stage of the power amplifier. While stability of the circuit was significantly improved along with high linearity at high input power levels, the power added efficiency (PAE) has been substantially sacrificed. Alternative and more sophisticated circuit design techniques need to be employed to maintain both high linearity and high power added efficiency. The MMIC circuits are fabricated

with heterostructure HBT wafers identical to those used to fabricate discrete devices and by using identical lithography, lift-off and etching techniques. A fabrication process of the MMIC circuits similar to that described by Rieh *et al* [4] was used. The photomicrograph of the fabricated single-stage MMIC medium power amplifier is shown in Fig. 6. The use of lumped passive elements has resulted in a small form factor of about 0.6 mm^2 chip area. It is noted that further reduction of chip area is still feasible using proper valued inductors.

V. POWER AMPLIFIER PERFORMANCE

The MMIC power amplifier was measured on-wafer under continuous wave (CW) operation (class AB) and no wafer thinning or extra heat sinking was employed. Fig. 7 shows the measured small-signal gain and input/output return losses of the power amplifier. At 8 GHz and with a bias of $I_E = -90 \text{ mA}$ and $V_{CB} = 7 \text{ V}$, the small-signal gain is 8.98 dB, with input and output return loss of 5.7 dB and 5.0 dB, respectively. These values vary with bias and the goal of these measurements was to optimize the matching at both input and output.

Fig. 8 shows the measured output power, gain and power added efficiency (PAE) as a function of input power, measured at 8 GHz, with the HBT biased at $V_{CB} = 7 \text{ V}$ and $V_{EB} = -1.15 \text{ V}$ (class AB). The linear power gain is as high as 9.7 dB with nearly 20 dBm of linear output power P_{out} . The output power at the peak value of PAE (16%) is 21.2 dBm (133 mW) and 23.4 dBm (219 mW) in its saturation.

A two-tone test was performed at 8 GHz with frequencies of two signals separated by 2 MHz using Tektronix 2754 spectrum analyzer. Low distortion with 3rd order intermodulation (IM) suppression C/I of -13 dBc at output power of 21.2 dBm, 16% PAE, and a bias voltage, V_{CB} , of 7 V is measured and shown in Fig. 9. The measured output third order intercept point (OIP3) is over 20 dBm. These results demonstrate the potential of medium power level amplification using SiGe HBTs with reduced form factor for short-range wireless communications at X band frequencies. It is noted, however, that much better power amplifier performance than presented

in this study can be achieved by using industry SiGe BiCMOS with smaller feature size, further optimization of SiGe HBT structures, and employing higher quality passive components. Regardless of these potential improvements, this study has demonstrated the feasibility of efficient X-band power amplification using SiGe HBTs with proper device design and operation configuration. Further optimization of the SiGe HBT heterostructure will allow improved power performance and may allow SiGe power amplifiers to be used at higher frequencies. Furthermore, based on the demonstration of MMIC power amplifier, higher frequency (>5 GHz) and higher power (>1 W) MMIC power amplifiers on Si also seems possible.

VI. CONCLUSION

SiGe power HBTs operating at 8-10 GHz have been demonstrated using properly designed device structure and employing a proper operation configuration. It is illustrated that a box-type Ge profile with high Ge content can allow a high base doping level while still maintaining high breakdown voltages and without using submicron emitter stripes. The high doping level dramatically improves the power gain values of SiGe HBTs and makes the CB configuration more favorable for power amplification than CE configuration. High power performance has thus been achieved from SiGe HBTs at 8 and 10 GHz. Single-stage medium power amplifiers operating at 8 GHz has also been demonstrated using these SiGe HBTs.

ACKNOWLEDGEMENT

The authors wish to acknowledge the support provided by NSF under grant No. ECS 0323717.

REFERENCES

- [1] A. Keerti and A. Pham, "SiGe power devices for 802.11a wireless LAN applications at 5 GHz," *Electronics Letters*, vol. 39, no. 16, pp. 1218-1220, Aug. 2003.

- [2] Z. Ma, S. Mohammadi, P. Bhattacharya, L. P. B. Katehi, S. A. Alterovitz and G. E. Ponchak, "A high power and high gain X-band Si/SiGe/Si heterojunction bipolar transistor," *IEEE Trans. on Microwave Theory and Techniques*, Vol. 50, No. 4, pp. 1101-1108, April 2002.
- [3] Z. Ma and N. Jiang, "On the operation configuration of SiGe HBTs based on power gain analysis," *IEEE Transactions on Electron Devices*, Vol. 52, No. 2, pp. 248-255, February 2005.
- [4] J.-S. Rieh, L.-H. Lu, L. P. B. Katehi, P. Bhattacharya, E. T. Croke, G. E. Ponchak and S. A. Alterovitz, "X- and Ku-band amplifiers based on Si/SiGe HBT's and micromachined lumped components," *IEEE Trans. Microwave Theory Tech.*, vol. 46, May 1998, pp. 685-694.

Figure Captions:

Figure 1. Measured SIMS profile in a CVD-grown heterostructure.

Figure 2. Photomicrograph of 10-finger SiGe/Si HBT.

Figure 3. Measured small-signal power gain characteristics of 10-emitter finger SiGe power HBTs ($A_E=600 \mu\text{m}^2$) in common-emitter and common-base configurations showing much higher power gain is available from common-based than common-emitter configuration. $BV_{CBO}=24\text{V}$.

Figure 4. Measured P_{out} , Gain and PAE of 20-finger CB SiGe/Si HBT at 10 GHz.

Figure 5. Measured P_{out} , Gain and PAE of 20-finger CB SiGe/Si HBT at 8 GHz.

Figure 6. Photomicrograph of a fabricated MMIC single-stage medium power amplifier with both input and output matching networks fabricated on chip (chip size: 0.6 mm^2).

Figure 7. Measured small-signal performance of single-stage MMIC power amplifier with 8.98 dB gain at 8 GHz. The input and output return losses are 5.7 dB and 5.0dB, respectively, at the same frequency.

Figure 8. Measured power performance of the SiGe HBT single stage MMIC power amplifier biased at $V_{CB} = 7\text{V}$ and $V_{EB} = -1.15\text{V}$. 21.24 dBm output power at peak efficiency (16%) and 23.4 dBm in saturation were obtained.

Figure 9. Measured two-tone linearity characteristics of single-stage SiGe HBT MMIC medium power amplifier at 8 GHz. OIP3 is over 20dBm.

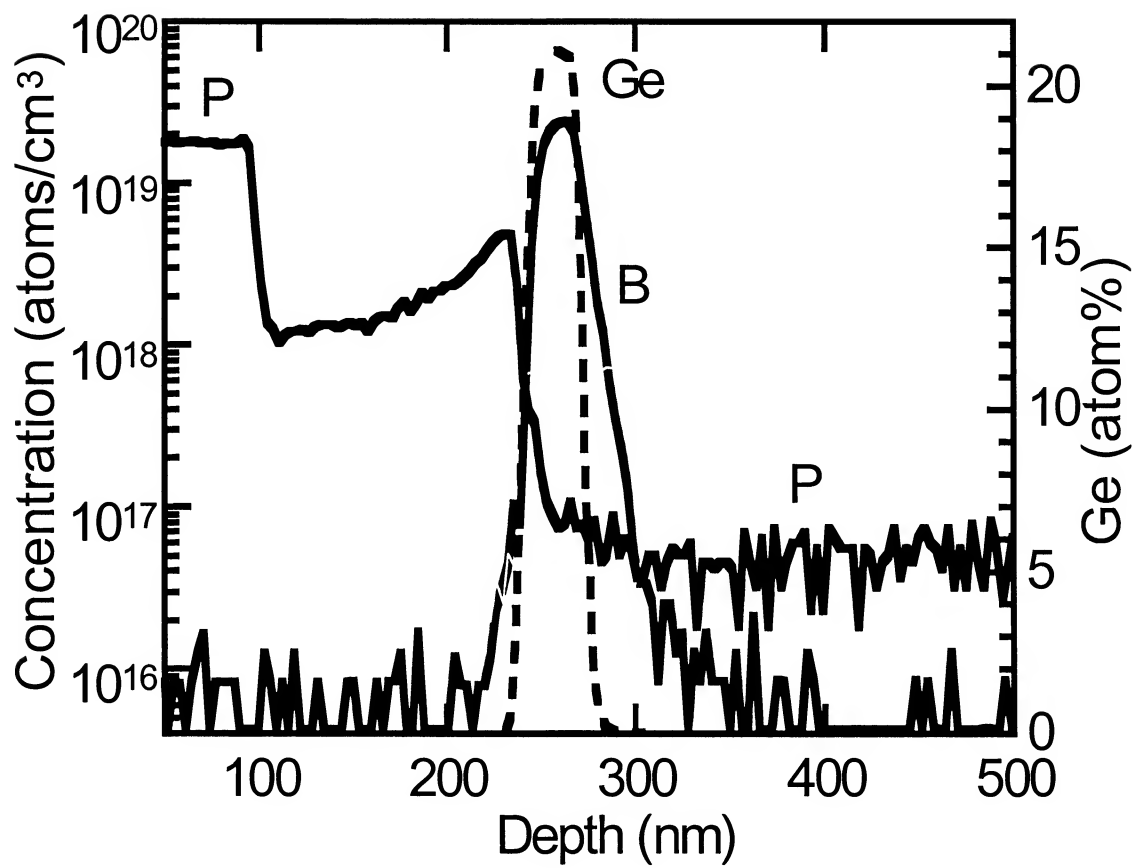


Figure 1, Z. Ma, *et al.*

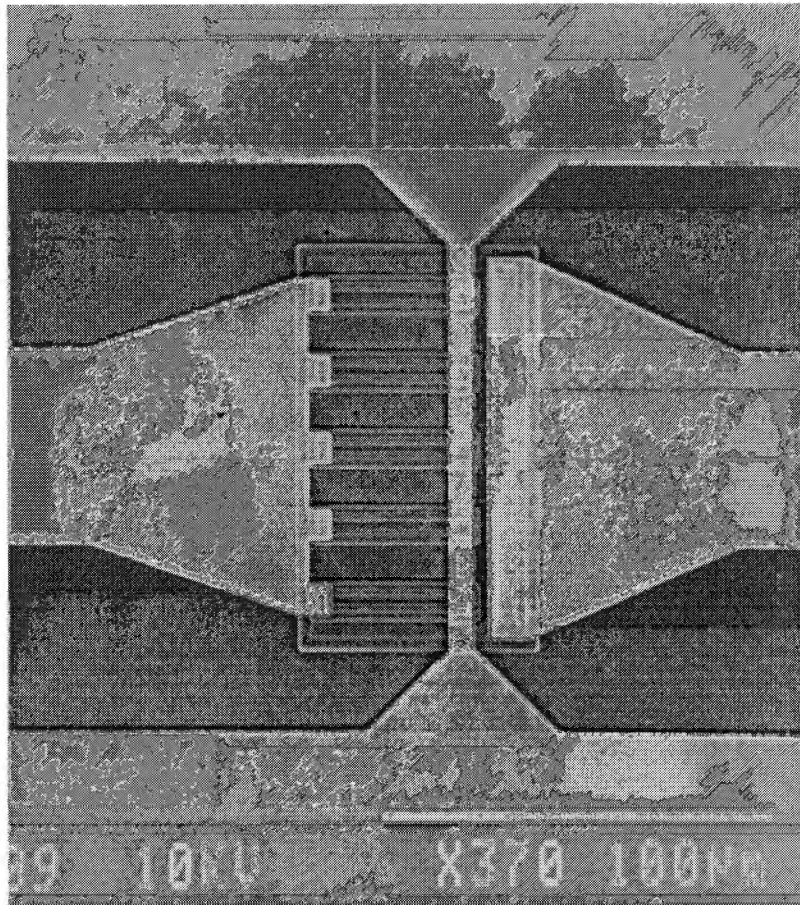


Figure 2, Z. Ma, *et al.*

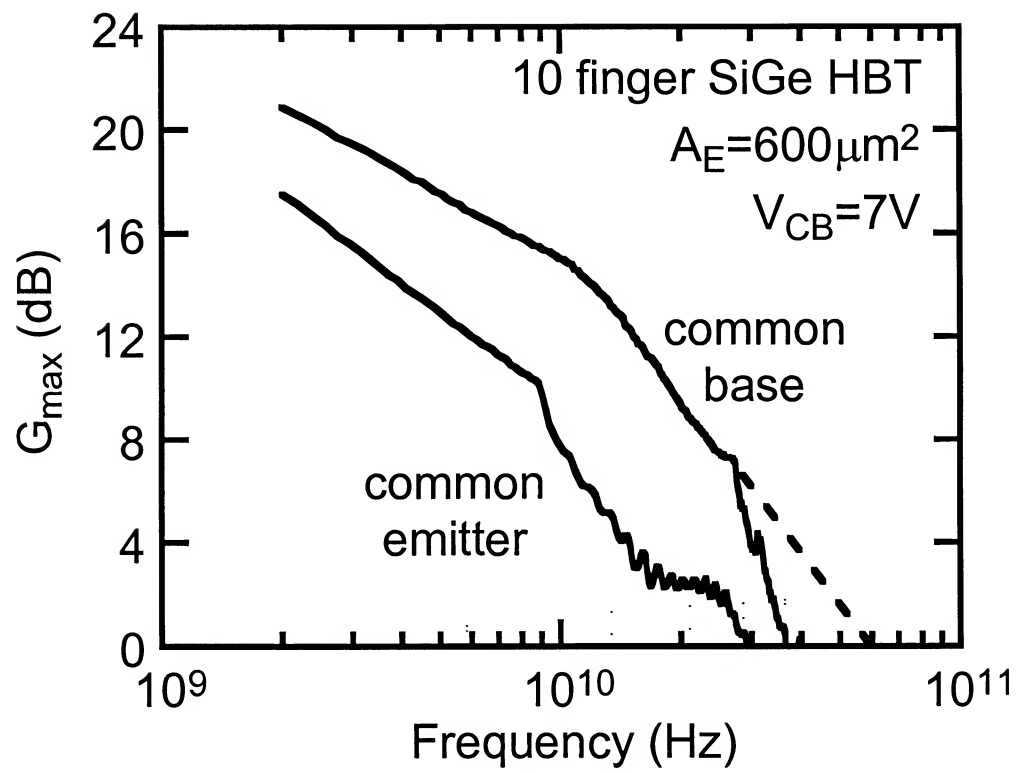


Figure 3, Z. Ma, *et al.*

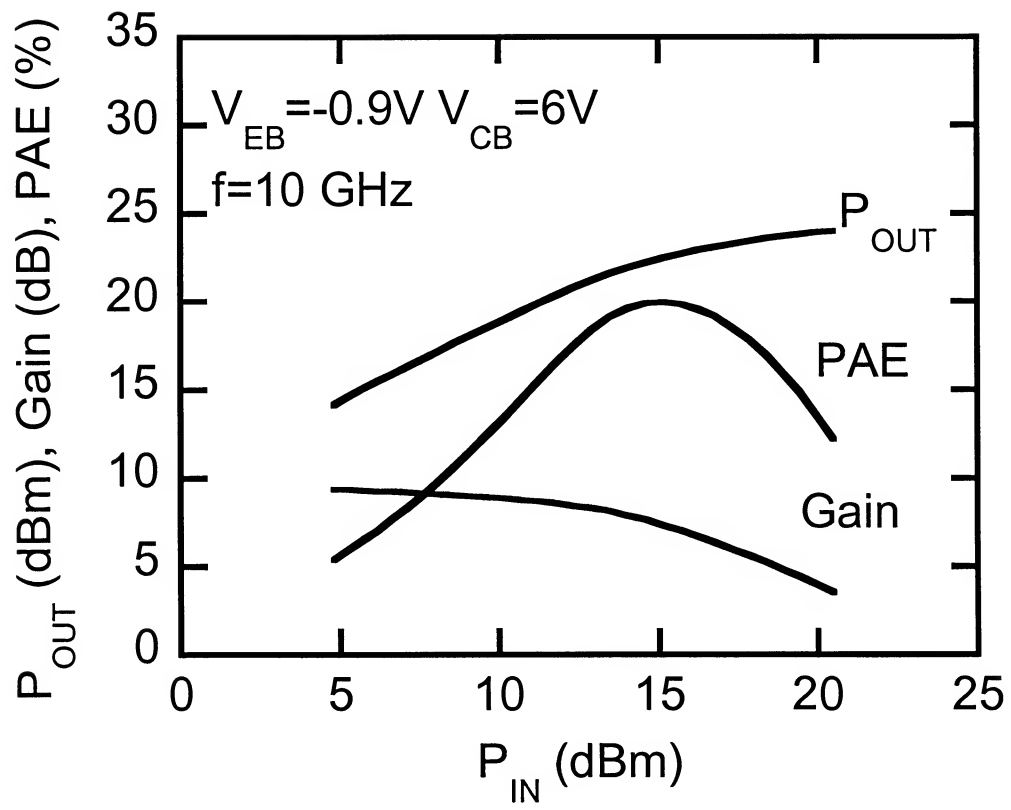


Figure 4, Z. Ma, *et al.*

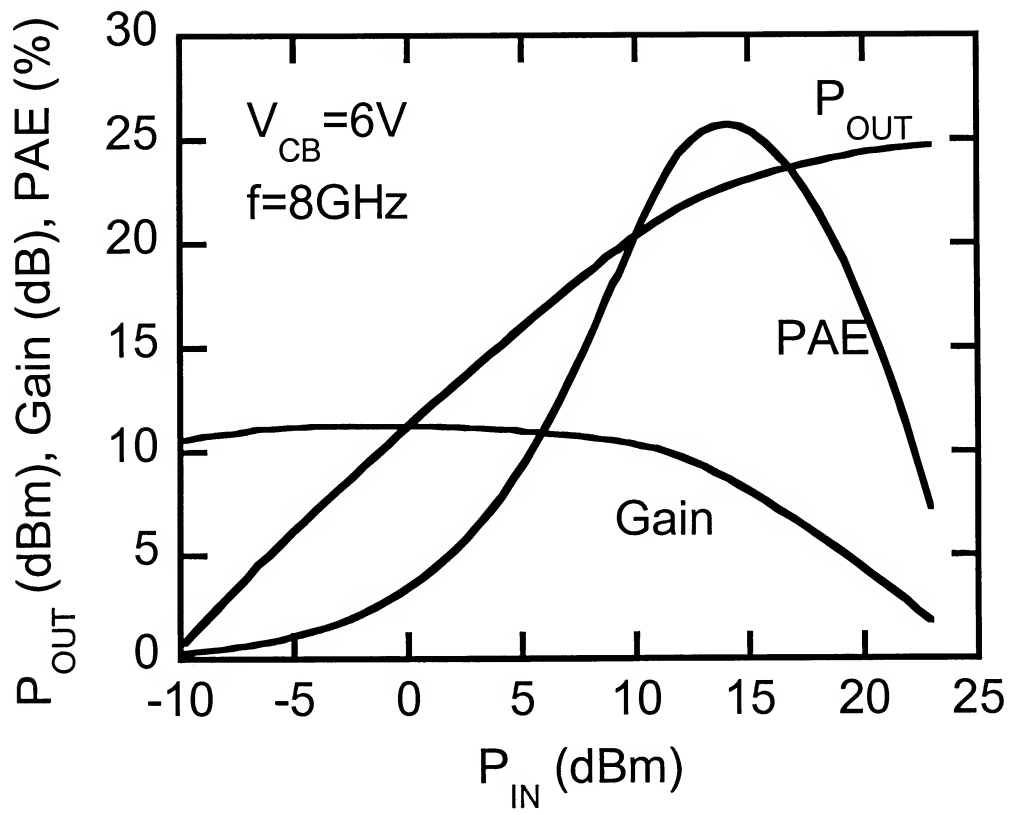


Figure 5, Z. Ma, *et al.*

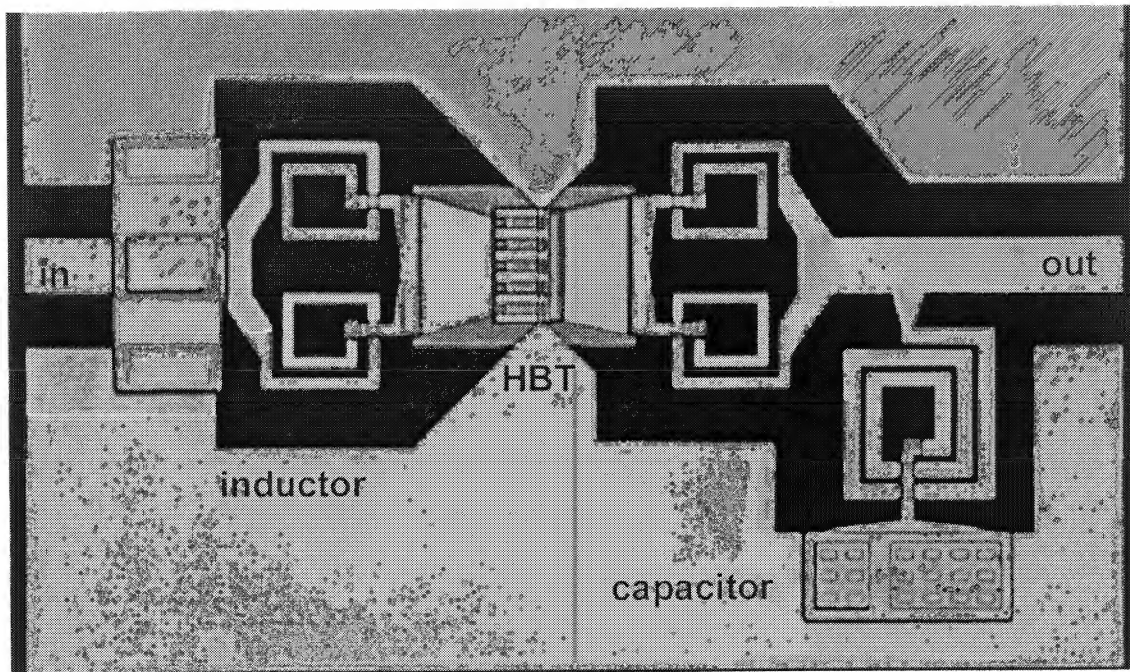


Figure 6, Z. Ma, *et al.*

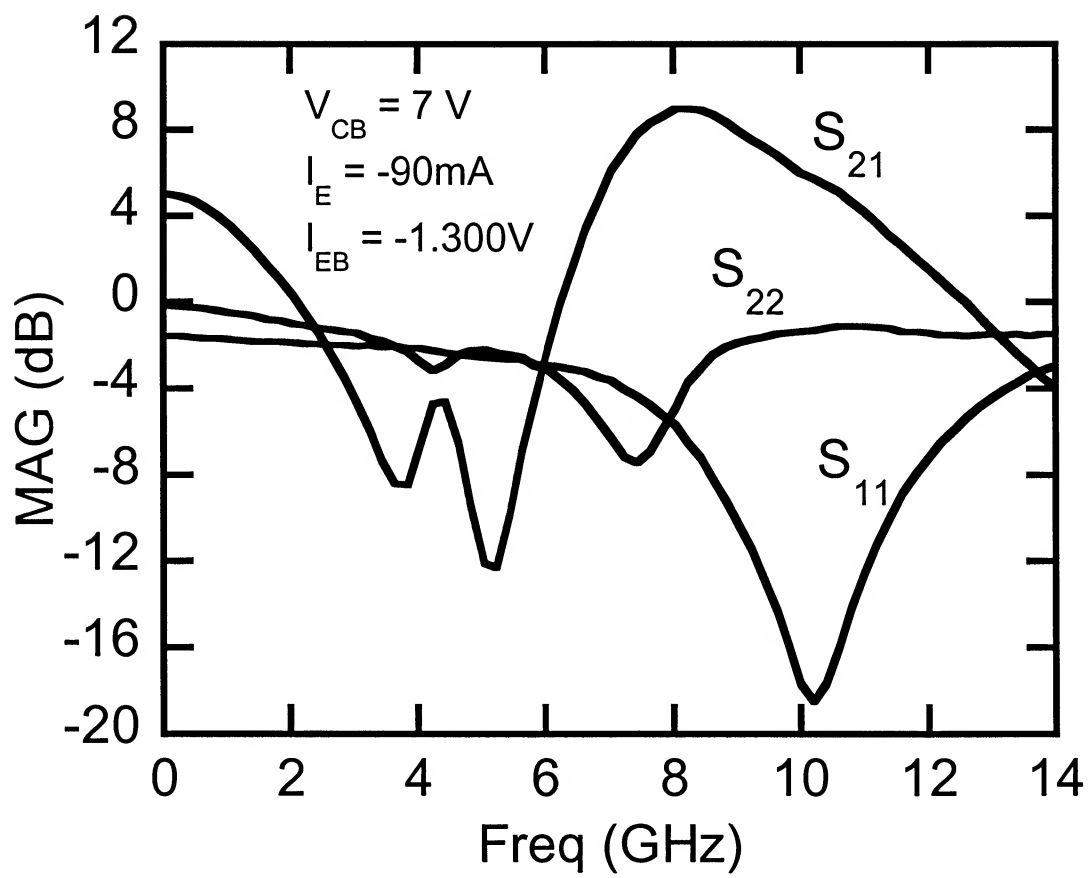


Figure 7, Z. Ma, *et al.*

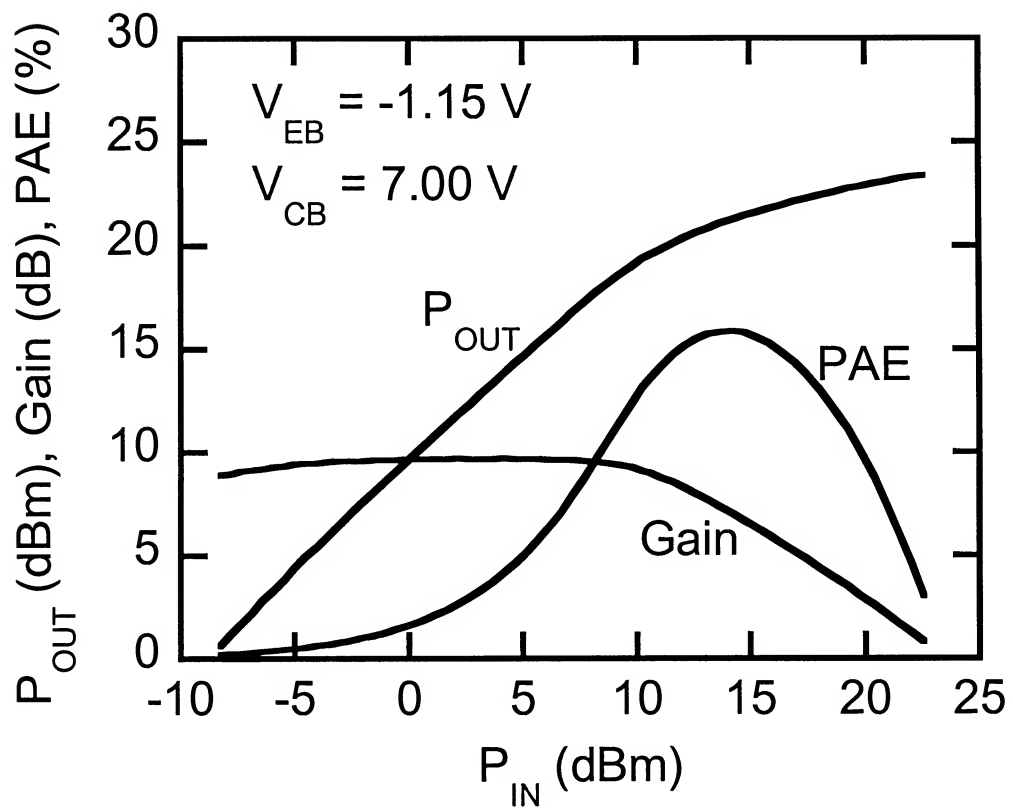


Figure 8, Z. Ma, *et al.*

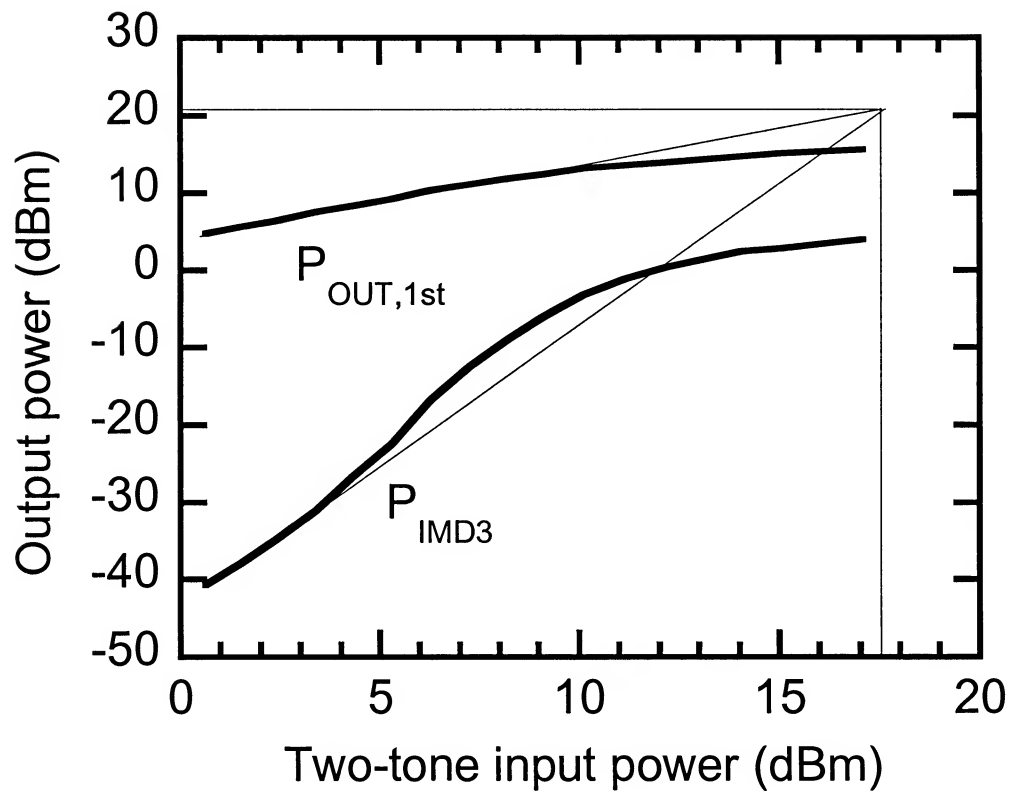


Figure 9, Z. Ma, *et al.*